Published in Proceedings World Geothermal Congress, session 14, 1426, 1-12, 2010
which should be used for any reference to this work

Validation of Chemical and Isotopic Geothermometers from Low Temperature Deep Fluids of Northern Switzerland

Romain Sonney and François-D. Vuataz
Centre for Geothermal Research – CREGE, University of Neuchâtel, Switzerland; romain.sonney@crege.ch

Keywords: Geothermometers, geothermal fluids, reservoir temperature, deep boreholes, geology, Northern Switzerland.

ABSTRACT

During more than 30 years, chemical and isotopic geothermometers have been extensively used to calculate and estimate the temperature of geothermal reservoirs in various geological, petrographical and thermal conditions. In this evaluation, chemical analyses of deep boreholes from the Molasse Basin and the Tabular Jura in Northern Switzerland were used to estimate reservoir temperatures with geothermometers, and results were compared to measured temperatures at depth. The presence of thermal waters in subhorizontal formations with a temperature range of 12-112°C, is associated with various geological and petrographical settings (sedimentary, crystalline rocks).

Composition of geothermal fluids depends on various and sometimes competing processes, such as full or partial chemical equilibrium, mixing with shallow groundwater or trapped seawater, dissolution of evaporite, ionic exchange with clays, or residence time in the reservoir. These processes are constraining for the application of geothermometers. Moreover, some of them have a limited temperature range of application cannot be used in some petrologic environments. Thus, a range of possible reservoir temperatures is calculated depending on several assumptions and compared to measured temperature. Application of chemical and isotopic geothermometers, using several calibrations proposed in the literature, is discussed in this specific context.

1. INTRODUCTION

Many different chemical and isotopic reactions might be used as geochemical thermometers or geothermometers to estimate reservoir temperature (Fournier, 1981). Geothermometers constitute one of the most important geochemical tool for the exploration and development of geothermal resources, and also during exploitation when monitoring the response of geothermal reservoirs to the production load (D'Amore and Arnorsson, 2000). They were developed from the mid-1960's to the mid-1980's and the most important ones are the silica (quartz and chalcedony), Na/K, Na-K-Ca. Others that have been developed are based on Na/Li, Li/Mg, K/Mg, Ca/Mg, Na/Ca, K/Ca ratios and Na-K-Mg relationships. Moreover, the geothermometer using the fractionation of oxygen isotopes between water and dissolved sulphate was tested. Gas and other isotope geothermometers were not employed in this paper, and therefore were not discussed.

Interpretation of results of these computations requires consideration of the geological and hydrogeological settings, and petrographical properties as well as complete chemical analyses of the sampled deep fluid (Fournier, 1981). Solute geothermometers are based on temperature-dependent mineral-fluid equilibria and their successful application relies on five basic assumptions (Fournier, 1977; Nicholson, 1993):

1) The concentration of the elements or species to be used in the geothermometer is controlled only by a temperature-dependent mineral-fluid reaction.

2) There is an abundance of the minerals and/or dissolved species in the rock-fluid system for the reaction to occur readily.

3) The reaction attains equilibrium in the reservoir or aquifer.

4) There is rapid flow to the surface with no re-equilibration after the fluid leaves the reservoir, ie. no near-surface reactions. In this paper, this condition does not occur because the studied deep fluids are subjected to lateral flows or are trapped in subhorizontal formations. Moreover, the deep fluids come from boreholes and not springs.

5) There is no mixing or dilution of the deep fluid (this assumption can be circumvented if the extent of dilution/mixing can be evaluated).

In this paper, the main objective consists to test the applicability of geothermometers in low temperature deep aquifers (200-2000 m) from Northern Switzerland with known reservoir temperature from borehole measurements (12-112°C). This paper will emphasize that different geothermometers can be applied in different geological setting and temperature ranges. Concerned aquifers are described in the first section and are located in the Molasse Basin and the Tabular Jura of the Northern Switzerland.

2. GEOLOGICAL SEETING

In total, 62 water analyses from deep boreholes in 16 geothermal sites were used to study the application of geothermometers. Their position on the simplified Swiss tectonic map can be subdivided into two areas (Figure 1). Some sites are located in the tectonic unit named Molasse Basin or Plateau whereas others are situated close to the Rhine River between the northeastern part of the Jura range in Switzerland and the Black Forest in Germany. This large area is characterized by a high geothermal gradient and a significant heat flow anomaly which can exceed 150 mW/m^2 (Rybach et al., 1987). For this reason, this area was regarded since decades as a zone of geothermal interest, and other boreholes exist but were not selected due to the absence of water analyses. Moreover, sites with ascending thermal springs located in the folded Jura between the Tabular Jura and the Molasse Basin were not taken into account. Indeed, the study of the application of geothermometers requires selecting sites where reservoir

depth is known, what is often difficult to identify for sites with ascending thermal fluids.

Geologically, Switzerland can be divided into three main parts: 12.5% of its surface lies in the Jura, 30.5% in the Molasse Basin and 57% in the External and Pennine Alps (Figure 1). The Jura can be also subdivided into two domains: the folded and the tabular Jura. The folded Jura extends from Geneva to Basel and consists of a succession of SW-NE folded chains, whereas the tabular Jura located at the south of the Rhine Valley contains subhorizontal formations which are slightly affected by tectonic events. In detail, the Tabular Jura consists of subhorizontal Mesozoic and Cenozoic cover rocks affected by Oligocene faulting overlapping a complex Hercynian basement (granite, gneiss) which outcrops in Germany (Back Forest). This sedimentary cover consists of an alternation of karstified limestones considered as aquifers and marls. At the bottom of the sedimentary cover, sandstones, quartzites and conglomerates are also present and can contain groundwater. Borehole investigations for geothermal prospection highlighted potential geothermal reservoirs from the Cretaceous to the Carboniferous. For the Jurassic formations, the Malm (upper) and Dogger (middle) karstified limestones with a variable thickness in the range of 200-500 m are separated by the Oxfordian marl.

The Triassic formations are unconformable with respect to the Permian and Carboniferous layers. They contain a greater variety of rocks than the Jurassic such as evaporite in the Keuper and Muschelkalk (Upper and Middle Triassic respectively), dolomite in the Muschelkalk and sandstone in the Buntsandstein (Lower Triassic). These rocks are considered as aquifers in addition to limestones which are also present, in particular in the Muschelkalk. Concerning the Permian and Carboniferous sediments, they are detrital deposits in old grabens inside the Hercynian basement. They are locally present in particular in a WSW-ENE band passing by Riniken and Weiach. In these two sites, boreholes crossed an alternation of sandstone, quartzite and silt with a thickness exceeding 1000 meters. More in the south (Schafisheim), the Buntsandstein sandstone of limited thickness directly overlies the Hercynian basement.

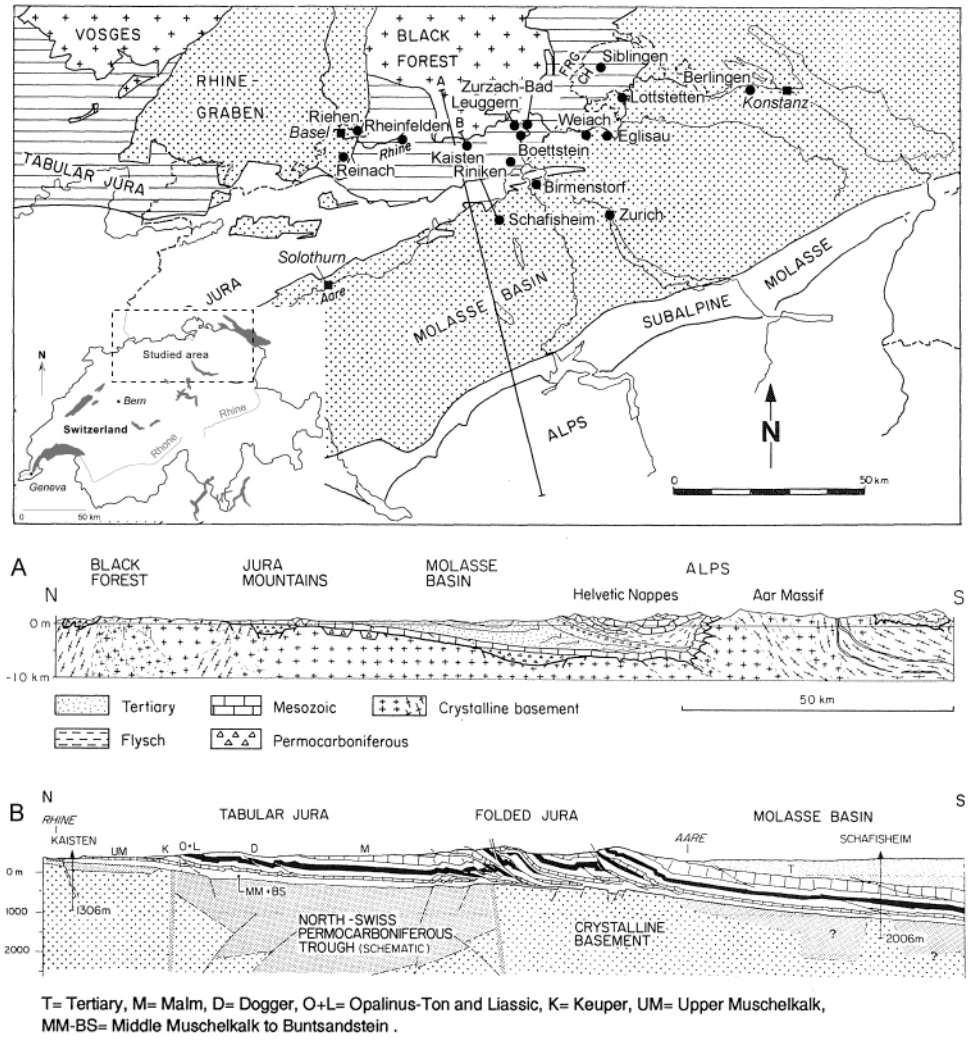

Figure 1: Map showing major structural units of Northern Switzerland and location of selected deep boreholes. Geological cross sections through Central and Northern Switzerland (A) and through Tabular and Folded Jura (B) (modified from Person et al., 1991).

On the southern part of the extremity of the Jura range, Cenozoic and Mesozoic formations are covered by Tertiary sediments of which the thickness increases towards the south and the Alps Mountains (Figure 1). This zone named Molasse Basin or Plateau has a hilly landscape, studded with lakes and with a few large plains. The Tertiary deposits, which stratigraphically overlie the Cenozoic and Mesozoic formations that are found in the tabular Jura, consist of three units: Lower Marine Molasse, Lower Fresh-water Molasse and Upper Marine Molasse (Trümpy, 1980). Groundwater flow is often absent in the Lower Fresh-water Molasse; it is therefore regarded as an aquiclude. Groundwater flow through the Upper Marine Molasse sandstone is common but dependent on local conditions. The geological formations of the Muschelkalk, Dogger and Malm beneath the Tertiary deposits represent the most important aquifers, and can contain great quantities of hot water in permeable fractures (Balderer, 1990).

Selected boreholes crossed the described aquifers at different depths due to the weak dip of layers towards the south. Some of boreholes reached the basement and samples and measurements were carried out on water inflows. The measured temperatures at depth at different sampling elevations highlight a geothermal gradient in the range 30-40°C/km from an average temperature at the surface fixed at 10°C (Figure 2). This result was already highlighted by Rybach (1992) in the study of the geothermal potential of the Swiss Molasse Basin. Some samples can be locally subjected to the rise of deep fluids from fractures or to mixing process with shallow groundwater due to their position beyond the gradient 30-40°C/km. The highest temperature at depth was measured at 112°C in the crystalline basement for the 2.3 km deep borehole at Weiach.

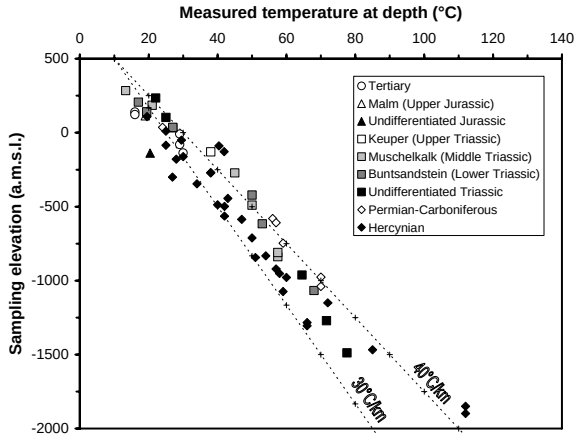

Figure 2: Plot of sampling elevation vs. measured temperature at depth for the studied deep fluids in boreholes. Deep fluids were subdivided into different symbols showing their geological setting. Two temperature gradient lines were added from an annual average air temperature around 10°C at the surface.

3. WATER CHEMISTRY

Many reports and publications concern the chemistry of geothermal fluids in formations of the sedimentary cover and its crystalline basement below. Chemical data of selected sites are given in Table 1 and are interesting from a geothermal point of view, because their temperature, mineralization and geological setting give information on potential geothermal reservoir. Their position on the Piper diagram (Figure 3) in relation to their geological formations indicates that different geochemical types of geothermal fluids occur. The geochemical type is defined by the most important cations and anions. Moreover, the Total Dissolved Solids (TDS) of waters tends to increase with depth, and a difference of TDS is visible between waters in the crystalline basement and waters from sedimentary formations which have higher TDS (Figure 4). In the following subsections, the different types of geothermal fluids are described in terms of geochemistry.

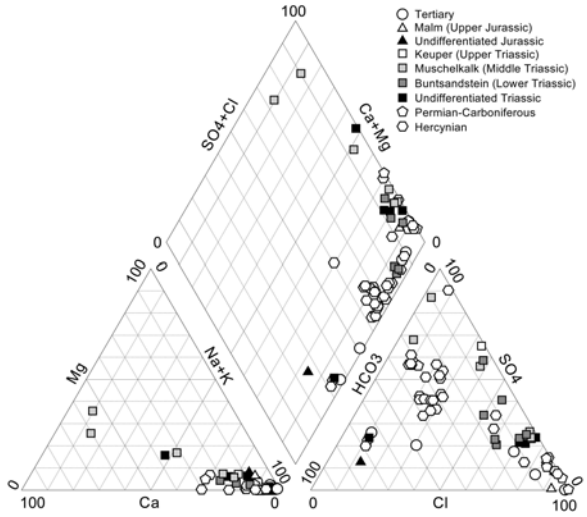

Figure 3: Piper diagram of deep fluids in Northern Switzerland. Data used are listed in Table 1.

3.1. Ca-SO_4 waters

Two selected sites at Leuggern and Weiach have a Ca-SO_4 type water with a TDS of 1.1 and 3.3 g/L respectively. Measured temperatures for this type are 13 and 50°C. This water was met in the fractured Muschelkalk limestone and is influenced by the dissolution of sulphate minerals (mainly gypsum and anhydrite) contained in the Triassic sediments. Gypsum and anhydrite are quickly dissolved and therefore, the Ca-SO_4 fingerprint is easily acquired by shallow or deep groundwaters upon interaction with these rocks. This lithotype is also found in the Jura range and the Alps due to the occurrence of Triassic rocks, which are often found in thrust faults and are locally present at shallow depth.

3.2. Na-HCO_3 waters

Sampled Na-HCO_3 waters were often met in the selected boreholes and have a TDS lower than 1.4 g/L except for the mineralized waters of the Rheinfelden well (TDS = 4.2 g/L). Measured temperatures for this type are in the range 20-66°C, and this water mainly circulates in crystalline rocks. Their mineralization is relatively weak compared to other water types which are up to 1 g/L (Figure 4). The sodium concentration of Na-HCO_3 waters is related to reactions with feldspars in crystalline rocks. In the Tertiary deposits of the Molasse Basin, Na-HCO_3 waters were pumped in the Lower Marine Molasse with temperature and TDS close to 29°C and 1 g/L respectively (Berlingen and Zürich). Two other Na-HCO_3 waters were respectively sampled in the Jurassic (20°C, 0.9 g/L) and Triassic (22°C, 0.6 g/L) formations of the tabular Jura at Lottstetten and Siblingen.

3.3. Na-SO_4 waters

Five selected waters in the basement at Kaisten, Leuggern and Weiach have a Na-SO_4 type water and a TDS in the

range 1-1.4 g/L except for one mineralized water (TDS = 4.9 g/L). These waters circulate in crystalline rocks, their sulphate concentration is due to the dissolution of sulphide minerals or anhydrite veins and their sodium comes mainly from reactions with feldspars. Four Na-SO_4 waters were analyzed in the Muschelkalk, Buntsandstein and Permian-Carboniferous formations with higher mineralization reaching 15 g/L, strongly influenced by the dissolution of Triassic evaporite.

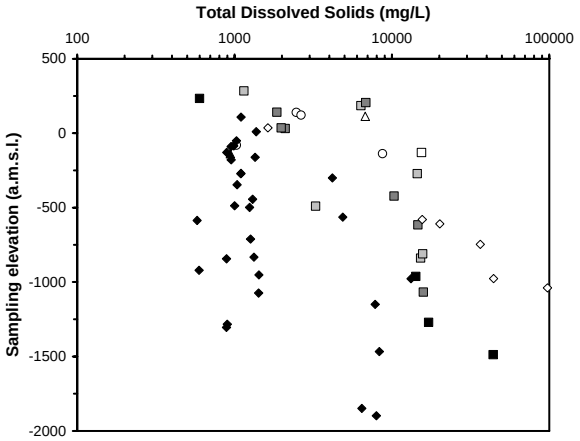

Figure 4: Sampling elevation vs. Total Dissolved Solids (see legend of symbols in Figure 2).

3.4. Na-Cl waters

Thermal Na-Cl waters have generally a high mineralization (TDS > 1 g/L) with concentrations sometimes exceeding 10 g/L, as in Weiach (97 g/L) or Reinach (44 g/L). Measured temperatures at depth for 29 sampled Na-Cl waters from 10 sites are in the range 16-112°C for any geological formations and any depth. The origin of this fingerprint is twofold. It could be due to the mixing of old, deep, strongly mineralized seawater and fresh water at different depths as observed in the crystalline basement and the Tertiary deposits (Chloride/Bromide molar ratio lower than the ocean line in Figure 5). Stober and Bucher (1999) studied deep groundwaters in the crystalline basement of the Black Forest region which is directly located in the north of the tabular Jura. They concluded that saline thermal waters used in spas have their origin in 3-4 km deep crystalline reservoirs and have developed their composition by mixing of surface freshwater with saltwater (of ultimately marine origin), and by water-rock reactions with an increasing mineral dissolution due to the presence of CO_2. Concerning thermal waters in the sedimentary cover below the Tertiary rocks, dissolution of halite deposits, locally present in the Triassic formations, generates high Na-Cl contents in water with Chloride/Bromide molar ratio up to the ocean line (Figure 5).

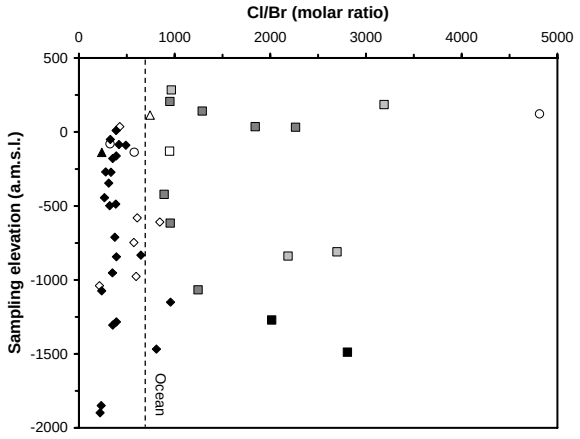

Figure 5: Sampling elevation vs. Chloride/Bromide molar ratio (see legend of symbols in Figure 2).

4. WATER GEOTHERMOMETERS

A series of geothermometers based on a temperature-dependent fluid-mineral equilibrium and an assemblage of minerals has been applied to deep groundwaters contained in subhorizontal formations of Northern Switzerland. Equations of geothermometers were represented on plots by curves and their variations with temperature could be compared to the measured temperature at depth for sampled waters. Measured temperature refers to the aquifer temperature from which the sample was taken, directly measured during the sampling campaign or estimated from the geothermal gradient in the borehole. Temperatures illustrated in this paper are as representative as possible of the average temperature of the sampled aquifer. The approach based on the comparison on measured/calculated temperature is useful to evaluate the applicability of geothermometers for low temperature. To clarify the discussion about the applicability of the geothermometers, this chapter is divided into sections referring to a specific geothermometer.

4.1 Silica geothermometers

The silica phases present in geothermal fluids are quartz, chalcedony and amorphous silica (D'Amore and Arnorsson, 2000). The total dissolved silica in selected waters and measured temperature at depth were plotted and curves representing equations of geothermometers were added (Figure 6). The dispersion of points indicates that geothermal fluids are often strongly affected by mixing processes with either shallow groundwaters containing low silica concentrations or trapped seawater. Therefore, the silica content of the discharged mixed water is usually below the reservoir concentration, and silica temperatures are therefore underestimated. Various petrographical properties of rocks met at depth are also at the origin of under-balanced dissolved silica concentrations analysed in geothermal fluids.

A general tendency to the increase of dissolved silica with temperature is observed, which follows the curves D of the two geothermometers using chalcedony (Fournier, 1977 and Arnorsson et al., 1983). For reservoir temperatures lower than 120-160°C, conditions present in the studied region, chalcedony has a higher solubility than quartz and controls silica concentrations in solutions (Arnorsson, 1975; Nicholson, 1993). Fournier (1981 and 1977) specifies that below 100°C, geothermal fluids may remain supersaturated with respect to quartz for years, and therefore the quartz

geothermometer works best in the temperature range 150-225°C.

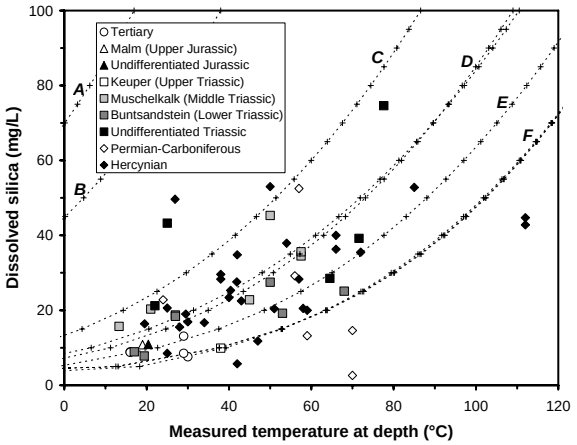

Figure 6: Dissolved silica vs. measured temperature at depth of deep fluids in Northern Switzerland. Curves correspond to selected silica geothermometers. A: amorphous silica; B: cristobalite β; C: cristobalite α (A to C: Fournier, 1977); D: chalcedony (Fournier, 1977 and Arnorsson et al., 1983); E: quartz (Arnorsson et al., 1983); F: quartz (Fournier, 1977; Truesdell, 1976; Fournier and Potter, 1982 and Verma and Santoyo, 1997).

4.2 Na-K geothermometer

The Na-K geothermometer was initially developed to locate the major upflow in high enthalpy geothermal systems, because a general decrease in Na/K ratios of geothermal fluids with increasing temperatures was observed (D'Amore and Arnorsson, 2000). This geothermometer is related to the variation of sodium and potassium in thermal waters due to ion exchange of these elements between co-existing alkali feldspars (Nicholson, 1993). Na-K equations are adapted for reservoir temperatures in the range 180-350°C (Ellis, 1979), but are limited at lower temperatures, notably less than 120°C (Nicholson, 1993) as illustrated in Figure 7.

Ion exchange between feldspars is limited for groundwaters of the sedimentary formations covering the basement because rocks are carbonates, evaporites or detrital deposits. The source of sodium and potassium comes from other minerals such as clays, seawater and precipitated minerals from seawater evaporation. Consequently, these two elements are not controlled by the feldspar ion-exchange reaction, and associated points on the plot in Figure 7 representing Na/K vs. measured temperature at depth are widely dispersed. Concerning selected data in the crystalline basement, values of Na/K ratios are better correlated with a general tendency to the decrease of Na/K ratios with temperature and thus depth.

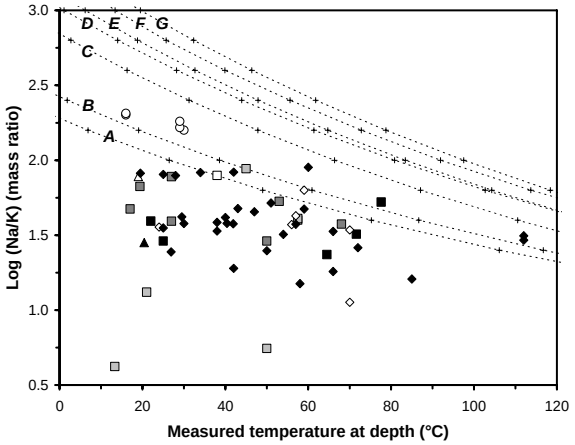

Figure 7: Log (Na/K) vs. measured temperature at depth of deep fluids in Northern Switzerland (see legend of symbols in Figure 6). Curves correspond to Na-K geothermometers. A: Truesdell, 1976; B: Arnorsson et al., 1983; C: Nieva and Nieva, 1987; D: Fournier, 1979; E: Verma and Santoyo, 1997; F: Arnorsson et al., 1998; G: Giggenbach, 1988.

4.3 Na-K-Ca geothermometer

The Na-K-Ca geothermometer, developed by Fournier and Truesdell (1973), does not give high and misleading results for cold and slightly thermal, non-equilibrated waters (D'Amore and Arnorsson, 2000), compared to the Na/K geothermometer which generally gives very high calculated temperatures for low enthalpy systems when geothermal fluids have high calcium contents (Nicholson, 1993). The Na-K-Ca geothermometer is also based on ion-exchange reactions between feldspars. As discussed above, the source of sodium, potassium and calcium in studied groundwaters comes from other geochemical processes, and they are not controlled by the feldspar ion-exchange reaction, and as observed for the Na/K geothermometer, estimated temperatures systematically over-estimate measured temperatures at depth (Figure 8).

Falsely high temperatures were estimated by the Na-K-Ca geothermometer, as shown in Figure 8, when applied to low-temperature reservoirs (< 120°C) relatively rich in magnesium. The geothermometer using magnesium correction developed by Fournier and Potter (1979) was applied to the studied groundwaters. Due to specific conditions described in the formulas of Fournier and Potter (1979), only some fluids were subjected to the magnesium correction (Figure 9). The reason is related to various magnesium concentrations in geothermal fluids, lower than 1 mg/L generally for waters in the crystalline basement and mostly up to 10 mg/L for carbonated aquifers containing dolomite (especially for the Triassic formations).

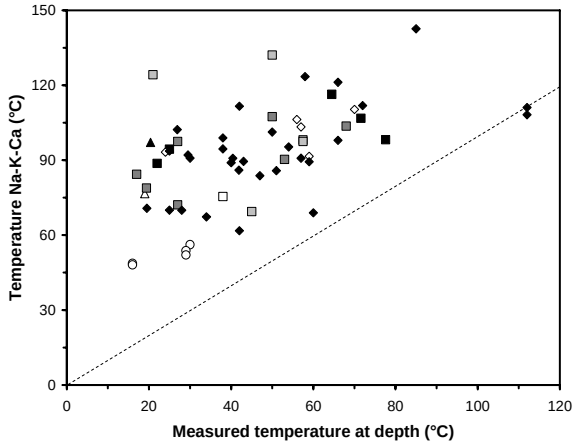

Figure 8: Computed temperature with Na-K-Ca geothermometer of Fournier and Truesdell (1973) vs. measured temperature at depth of deep fluids in Northern Switzerland (see legend of symbols in Figure 6).

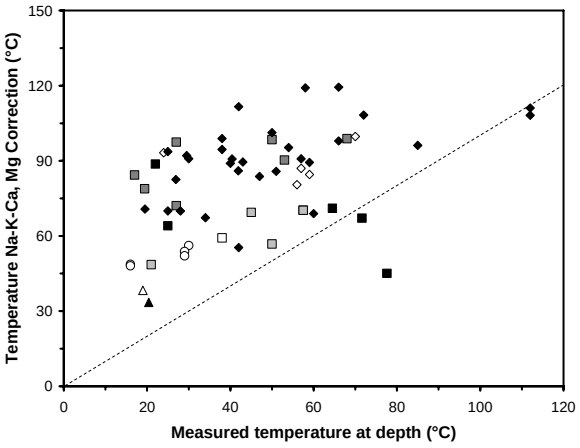

Figure 9: Computed temperature with Na-K-Ca geothermometer using magnesium correction of Fournier and Potter (1979) vs. measured temperature at depth of deep fluids in Northern Switzerland (see legend of symbols in Figure 6).

4.4 Na-K-Mg geothermometer

Selected data of geothermal fluids in Northern Switzerland were plotted in the ternary diagram of Giggenbach (1988) to estimate reservoir temperature and to recognize groundwaters which have attained equilibrium with the host lithologies (Figure 10). Corresponding groundwaters plot below the full equilibrium curve which determines variations of the Na/K geothermometry equation of Giggenbach (1988). Therefore, these groundwaters are not suitable for Na/K geothermometry as shown previously. Points representing groundwaters are shifted towards the magnesium vertex indicating that waters are partially equilibrated or mixed. Dilution and mixing coupled to water-rock interactions in studied heterogeneous geological formations are processes limiting the application of these types of ionic solute geothermometers.

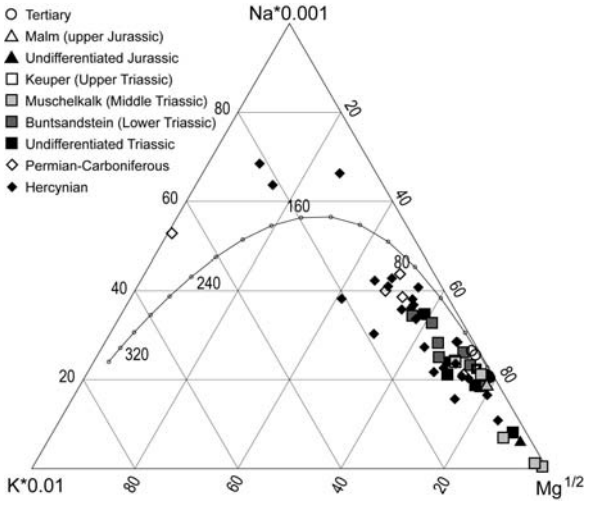

Figure 10: Giggenbach diagram of deep fluids in Northern Switzerland. Used data are listed in Table 1. The line on the ternary plot represents the full equilibrated line determined by variations of the Na/K geothermometry equation of Giggenbach (1988).

4.5 Other cation geothermometers

4.5.1 K-Mg geothermometer

Two K-Mg geothermometers of Giggenbach (1988) and Fournier (1991) were applied to studied geothermal fluids to test their applicability. Data plotted in Figure 11 illustrate a trend to the increase of the K/Mg ratios with measured temperature at depth, but separated from curves which over-estimate temperature. Initially, the K-Mg geothermometer was developed in the same way as the Na-K geothermometer. D'Amore and Arnorsson (2000) explain that progressive interaction between water and rock towards equilibrium changes Na/K ratios towards equilibrium with feldspars, and similarly, magnesium concentrations decrease because magnesium is incorporated into precipitating minerals such as smectite and chlorite. These processes cause K/Mg ratios to increase strongly. The K-Mg geothermometer was first applied to waters from a low-enthalpy reservoir which had not attained equilibrium with alkali feldspars (Nicholson, 1993), as for the studied geothermal fluids which are partially equilibrated or mixed waters (Figure 10). However, data plotted in Figure 11 indicate that the K-Mg geothermometer is not appropriate because it over-estimates temperature. By considering only geothermal fluids in formations of the sedimentary cover which consist of carbonate, evaporite and detrital deposits, the K-Mg geothermometers cannot be applied. Indeed, these formations are poor in feldspars implying another origin for these elements such as dolomite dissolution, leaching of seawater brines, etc. Data plotted for sedimentary groundwaters are widely dispersed in Figure 11.

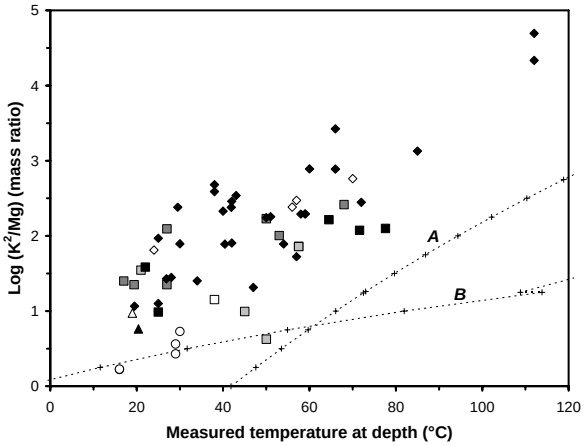

Figure 11: Log (K^2/Mg) vs. measured temperature at depth of deep fluids in Northern Switzerland (see legend of symbols in Figure 10). Curves correspond to K-Mg geothermometers. A: Giggenbach, 1988; B: Fournier, 1991.

4.5.2 Mg-Li geothermometer

The Mg-Li geothermometer was developed in the same way as the K-Mg geothermometer, resting on exchange reactions with magnesium, for waters from a low-enthalpy reservoir which had not attained equilibrium with alkali feldspars (Nicholson, 1993). Thereby, these processes cause Mg/Li ratios to decrease strongly, and conversely for K/Mg. The two equations of Kharaka et al. (1985) and Kharaka and Mariner (1989) were tested on the studied geothermal fluids but they strongly over-estimate temperature, especially for waters in the crystalline basement (Figure 12). Data plotted in Figure 12 show a general trend to the decrease of the Mg/Li ratios with measured temperature at depth. This tendency is better organized for crystalline thermal waters. Data plotted for sedimentary groundwaters are widely dispersed due to the occurrences of dilution and mixing processes and water-rock interactions which are more pronounced in sedimentary formations.

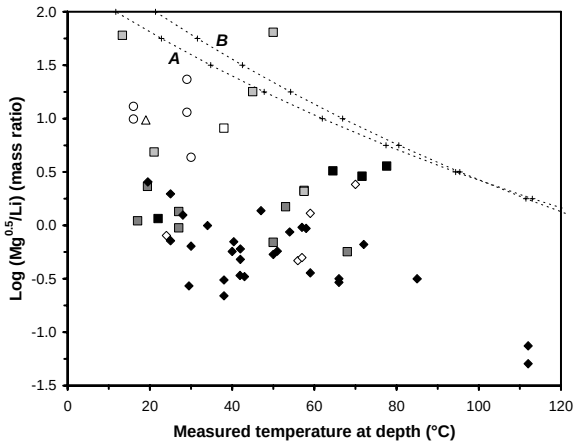

Figure 12: Log ($Mg^{0.5}$/Li) vs. measured temperature at depth of deep fluids in Northern Switzerland (see legend of symbols in Figure 10). Curves correspond to Mg-Li geothermometers. A: Kharaka et al., 1985; B: Kharaka and Mariner, 1989.

4.5.3 Na-Li geothermometer

The Na-Li geothermometer was initially developed by Fouillac and Michard (1981) from a statistic study about groundwaters in granitic and volcanic domains. Two other Na-Li geothermometers are documented in Kharaka et al. (1982) and Verma and Santoyo (1997) and were tested on the studied waters. These two other equations are relatively distant because they results from empirical calibration, based on data in selected geothermal fields. Data plotted in Figure 13 highlight two distinct features. The first relates to geothermal fluids in sedimentary formations where data are widely dispersed (Figure 13). Some geothermal fluids have high Na/Li ratios because sodium is enriched by the dissolution of halite and the leaching of trapped seawater. Frequently, waters in deep carbonate aquifers have low lithium contents (< 1 mg/L) what can also explain the strong ratios. The second concerns groundwaters in crystalline rocks which have generally lower Na/Li ratios due to higher lithium concentrations (> 1 mg/L). Moreover, Na/Li ratios remain relatively stable around 2.5 whatever the measured temperature at depth. The Na/Li geothermometer appears to be sensitive to the total dissolved solids of the water at depth, locally controlled by contributions of Na-Cl, and the rock type.

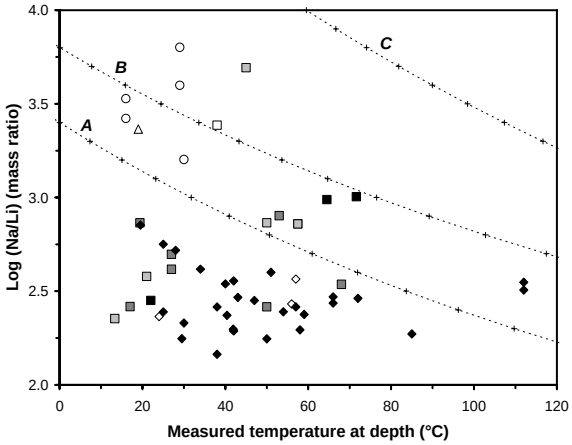

Figure 13: Log (Na/Li) vs. measured temperature at depth of deep fluids in Northern Switzerland (see legend of symbols in Figure 10). Curves correspond to Na-Li geothermometers. A: Verma and Santoyo, 1997; B: Fouillac and Michard, 1981; C: Kharaka et al., 1982.

4.5.4 Na-Ca and K-Ca geothermometers

The two Na-Ca and K-Ca geothermometers developed by Tonani (1980) were selected and tested on the studied waters. According to D'Amore and Arnorsson (2000), they have not been employed much for geothermal exploration, and they seem to be affected by CO_2 partial pressure. These geothermometers are also related to ion-exchange reactions between feldspars and, therefore, are suitable for equilibrated waters. Concerning the studied groundwaters, they give strongly over-estimated results (Figure 14). In this case, the mineral assemblages involved are different from those used for the calibration of these geothermometers, as it was already mentioned by Marini et al. (1986) for carbonate-evaporite geothermal reservoirs.

4.5.5 Ca-Mg geothermometer

The Ca-Mg geothermometer of Marini et al. (1986) was also taken into account and is specific for carbonate-evaporite geothermal reservoirs. Thereby, it was interesting to test this geothermometer for geothermal fluids in carbonate-evaporite aquifers of the Mesozoic sedimentary cover. The presence of dolomite in the sedimentary cover allows having thermal waters with magnesium

concentrations up to 1 mg/L, and thus, Ca/Mg ratios tend to decrease compared to crystalline waters poor in magnesium (< 1 mg/L). Data plotted of selected waters in Figure 15 show differences due to their geological setting. Points for the sedimentary cover are clearly closer to the Ca-Mg geothermometer than points representing crystalline waters.

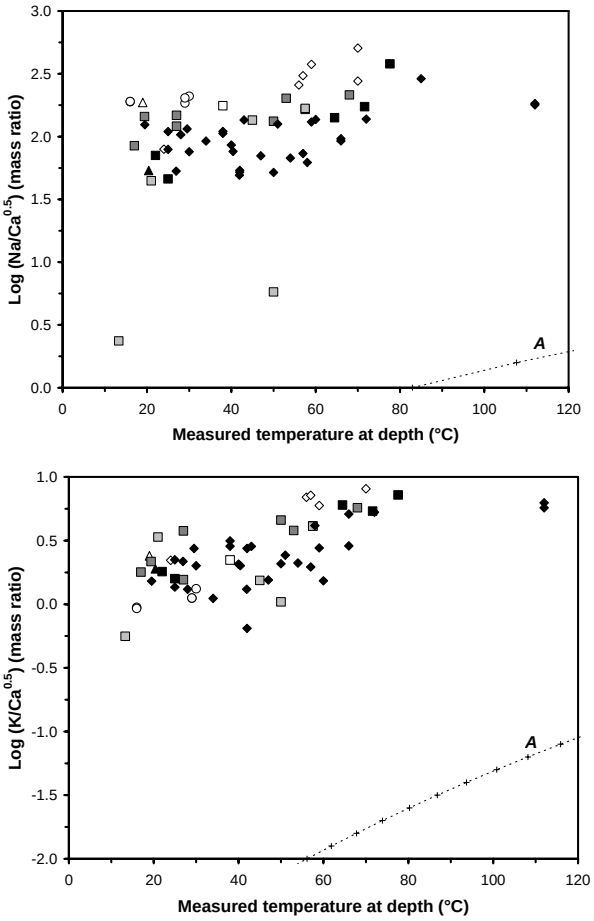

Figure 14: Log (Na/Ca$^{0.5}$) and log (K/Ca$^{0.5}$) vs. measured temperature at depth of deep fluids in Northern Switzerland (see legend of symbols in Figure 10). Curves A correspond to Na-Ca and K-Ca geothermometers of Tonani (1980).

4.6 Oxygen isotope geothermometer

The sulphate oxygen isotope geothermometer is based upon the experimental work of Lloyd (1968), who measured the fractionation of ^{16}O and ^{18}O between SO_4^{2-} and water at 350°C, as well as the work of Mizutani and Rafter (1969) who measured the ^{16}O and ^{18}O between water and HSO_4^- at 100 to 200°C (Fournier, 1981). Only the geothermometer of Mizutani and Rafter was applied to studied geothermal fluids (Figure 16).

In the case of geothermal fluids of northern Switzerland, various isotopic signatures of ^{18}O in water and sulphate are observed due to water-rock interactions and chemical processes in different geological domains. As observed for the Paris Basin in France (Fouillac et al., 1990), the sulphate in studied groundwaters has different origins: dissolution of evaporite (gypsum and anhydrite), oxidation of sedimentary sulphides in rocks and leaching of trapped seawater. For each case, isotopic values of ^{18}O in sulphate can be strongly different. Moreover, ^{18}O values of marine evaporite sulphate minerals vary with their geologic age due to changes in the isotopic composition of oceanic sulphate with time (Pearson et al., 1991). Concerning ^{18}O of water, a great difference in values can be caused by mixing processes with shallow groundwater or trapped seawater. All these processes in studied geothermal fluids induce that the oxygen isotope geothermometer is often not suitable. Data plotted in Figure 16 indicate that this geothermometer has the tendency to over-estimate temperature, especially for crystalline waters.

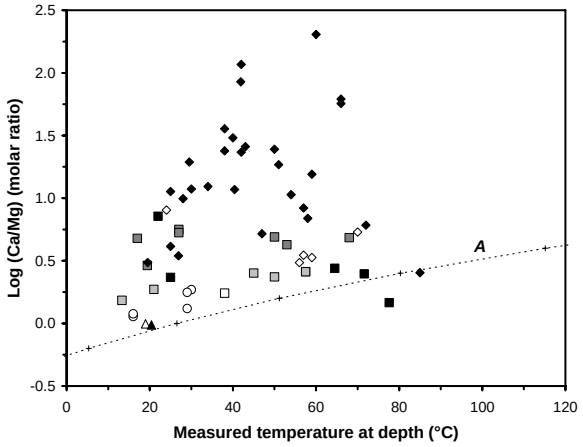

Figure 15: Log (Ca/Mg) vs. measured temperature at depth of deep fluids in Northern Switzerland (see legend of symbols in Figure 10). Curve A corresponds to Ca-Mg geothermometer of Marini et al. (1986).

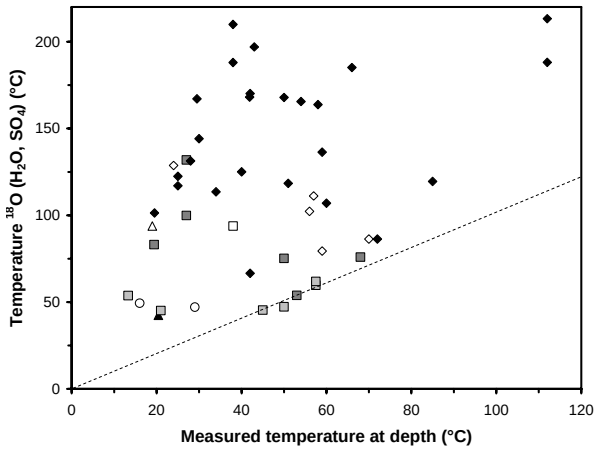

Figure 16: Computed temperature with oxygen isotope geothermometer of Mizutani and Rafter (1969) vs. measured temperature at depth of deep fluids in Northern Switzerland (see legend of symbols in Figure 10).

6. SYNTHESIS

Chemical and isotopic geothermometers were applied on chemical data and measured temperature at depth of geothermal fluids in boreholes from northern Switzerland, in the range of 12-112°C and considered as low-temperature geothermal systems. For each type of geothermometer, the method used was to plot measured temperature at depth with the corresponding geotemperature curves. Thereby, the accuracy and applicability of various geothermometers can be evaluated in these low-temperature geothermal systems.

For instance, there is some uncertainty in the interpretation of dissolved silica concentration in geothermal fluids

because the solid phase controlling dissolved silica is often unknown (quartz or chalcedony in general), mixing processes with shallow groundwaters and trapped seawater occur and water-rock interactions are difficult to identify. Consequently, the application of silica geothermometers often gives underestimated values even if the chalcedony geothermometer was shown to be the most accurate of these.

Cationic geothermometers using ratios between lithium, sodium, potassium, magnesium and calcium were also tested and obtained results largely overestimate the measured temperature at depth. Application of these geothermometers is more suitable for high-enthalpy systems (>150°C), containing groundwaters reaching equilibrium with feldspars and clay minerals. This assumption is fundamental for the use of the majority of cationic geothermometers, what is not verified for studied geothermal fluids, subjected to various chemical processes. Finally, the oxygen isotope geothermometer based on ^{18}O of water and sulphate did not give useful results, especially for crystalline thermal waters. The isotopic signature of ^{18}O in particular in sulphate depends of a lot on different origins from various geological domains. In conclusion, chemical and isotopic geothermometers can be applied in low temperature geothermal systems (< 100°C) with a much greater cautiousness than in high temperature systems (> 150°C). Indeed, chemical reactions or isotopic fractionation may not reach equilibrium in low temperature reservoirs during the underground transit time of the deep fluids. Mixing of various types of fluids in heterogeneous rocks composition does not favour a complete equilibrium. However, detailed rock and fluid geochemistry in a given geothermal exploration zone can alleviate the uncertainties in the use of geothermometers.

REFERENCES

Arnorsson, S.: Application of the silica geothermometer in low temperature area in Iceland, *American Journal of Science*, **275**, (1975), 763-784.

Arnorsson, S., Gunnlaugsson, E., and Svavarsson, H.: The chemistry of geothermal waters in Iceland. III. Chemical geothermometry in geothermal investigations, *Geochimica and Cosmochimica Acta*, **47**, (1983), 567-577.

Arnorsson, S., Andrésdottir, A., Gunnarsson, I., and Stefánsson, A.: New calibration for the quartz and Na/K geothermometers – valid in the range 0-350°C, *Proceedings*, Geoscience Society of Iceland Annual Meeting, (1998), 42-43.

Balderer, W.: Hydrogeologische Charakterisierung der Grundwasservorkommen innerhalb der Molasse der Nordostschweiz aufgrund von hydrochemischen und Isotopenuntersuchungen, *Steirische Beiträge zur Hydrogeologie*, **41**, (1990), 35-104.

Carlé, W.: Die Mineral- und Thermalwässer von Mitteleuropa. Geologie, Chemismus, Genese, Wissenschaftlicher Verlag, Stuttgart, Germany, (1975), 641p.

D'Amore, F., and Arnorsson, S.: Geothermometry. In: Arnorsson, S.: Isotopic and chemical techniques in geothermal exploration, development and use, International Atomic Energy Agency, Vienna, (2000), 152-199.

Ellis, A.J.: Chemical geothermometry in geothermal systems, *Geothermics*, **25**, (1979), 219-226.

Fouillac, R., and Michard, S.: Sodium/lithium ratio in water applied to geothermometry of geothermal reservoirs, *Geothermics*, **10**, (1981), 55-70.

Fouillac, C., Fouillac, A.M., and Criaud, A.: Sulphur and oxygen isotopes of dissolved sulphur species in formation waters from the Dogger geothermal aquifer, Paris Basin, France, *Applied Geochemistry*, **5(4)**, (1990), 415-427.

Fournier, R.O.: Chemical geothermometers and mixing models for geothermal systems, *Geothermics*, **5**, (1977), 41-50.

Fournier, R.O.: A revised equation for the Na/K geothermometer, *Geothermal Resources Council Transactions*, **3**, (1979), 221-224.

Fournier, R.O.: Application of water geochemistry to geothermal exploration and reservoir engineering. In: Rybach, L., and Muffler, L.J.P.: Geothermal systems: Principles and case histories, Wiley & Sons, Chichester, New York, Brisbane, Toronto, (1981), 109-143.

Fournier, R.O.: Water geothermometers applied to geothermal energy. In: D'Amore, F.: Application of Geochemistry in Geothermal Reservoir Development, United Nations Institute for Training and Research, Rome, (1991), 37-69.

Fournier, R.O., and Truesdell, A.H.: An empirical Na-K-Ca geothermometer for natural waters, *Geochimica and Cosmochimica Acta*, **37**, (1973), 1255-1275.

Fournier, R.O., and Potter, R.W.II.: Magnesium correction to the Na-K-Ca chemical geothermometer, *Geochimica and Cosmochimica Acta*, **43**, (1979), 1543-1550.

Fournier, R.O., and Potter, R.W.II.: A revised and expanded silica (quartz) geothermometer, *Geothermal Resourcse Council Bulletin*, **11(10)**, (1982), 3-12.

Giggenbach, W.F.: Geothermal solute equilibria. Derivation of Na-K-Mg-Ca geoindicators, *Geochimica and Cosmochimica Acta*, **52**, (1988), 2749-2765.

Gorhan, H.L., and Griesser, J.C.: Geothermische Prospektion im Raume Schinznach Bad – Baden, *Mater. Géol. Suisse, Série Géothechnique*, **76**, (1998), 73p.

Hauber, L.: Der Südliche Rheingraben und seine geothermische Situation, *Bull. Ver. Schweiz. Petroleum-Geol. U. Ing.*, **60(137)**, (1993), 53-69.

Högl, O.: Die Mineral- und Heilquellen der Schweiz, Haupt, Verlag, Bern, Switzerland, (1980), 302p.

Kharaka, Y.K., Lico, M.S., and Law, L.M.: Chemical geothermometers applied to formation waters, Gulf of Mexico and California Basins, *Bulletin of American Association of Petroleum Geologists*, **66**, (1982).

Kharaka, Y.K., Specht, D.J., and Carothers, W.W.: Low to intermediate subsurface temperatures calculated by chemical geothermometers, *American Association of Petroleum Geologists*, Annual meeting, New Orleans, **69**, (1985).

Kharaka, Y.K., and Mariner, R.H.: Chemical geothermometers and their application to formation waters from sedimentary basins. In: Naser, N.D., and McCollin, T.H.: Thermal History of Sedimentary Basin, Springer-Verlag, New York, (1989), 99-117.

Lloyd, R.M.: Oxygen isotope behavior in the sulphate water system, *Journal of Geophysical Research*, **73(18)**, (1968), 6099-6110.

Marini, L., Chiodini, G., and Cioni, R.: New geothermometers for carbonate-evaporite geothermal reservoirs, *Geothermics*, **15(1)**, (1986), 77-86.

Mizutani, Y., and Rafter, T.A.: Oxygen isotope composition of sulphates. Oxygen isotope fractionation in the bisulphate ion-water system, *New Zealand Journal of Science*, **12(1)**, 54-59.

Nicholson, K.: Geothermal fluids. Chemistry and exploration techniques, Springer-Verlag, Berlin Heidelberg, (1993), 263p.

Nieva, D., and Nieva, R.: Developments in geothermal energy in Mexico, Part 12. A cationic geothermometer for prospecting of geothermal resources, *Heat Recovery Systems & CHP*, **7**, (1987), 243-258.

Pearson, F.J., Lolcama, J.M., and Scholtis, A.: Chemistry and waters in the Böttstein, Weiach, Riniken, Schafisheim, Kaisten and Leuggern boreholes: A hydrochemically consistent data set, Technical Report 86-19, NAGRA, (1989), 102p.

Pearson, F.J., Balderer, W., Loosli, H.H., Lehmann, B.E., Matter, A., Peters, T., Schmassmann, H., and Gautschi, A.: Applied isotope hydrogeology. A case study in northern Switzerland, Elsevier, Amsterdam, Studies in Environmental Science, **43**, (1991), 439p.

Rybach, L.: Geothermal potential of the Swiss Molasse Basin, *Eclogae Geologicae Helveticae*, **85(3)**, (1992), 733-744.

Rybach, L., Eugster, W., and Griesser, J.C.: Die geothermischen Verhältnisse der Nordschweiz, *Eclogae Geologicae Helveticae*, **80**, (1987), 521-534.

Sonney, R., and Vuataz, F.D.: Properties of geothermal fluids in Switzerland: A new interactive database, *Geothermics*, **37**, (2008), 496-509.

Stober, I., and Bucher, K.: Deep groundwater in the crystalline basement of the Black Forest region, *Applied Geochemistry*, **14**, (1999), 237-254.

Tonani, F.B.: Some remarks on the application of geochemical techniques in geothermal exploration, *Proceedings*, Second Symposium Advances in European Geothermal Research, Strasbourg, (1980), 428-443.

Truesdell, A.H.: Summary of section III. Geochemical techniques in exploration, *Proceedings*, Second United Nations Symposium on the Development and Use of Geothermal Resources, San Francisco, (1976), 53-79.

Trümpy, R.: An outline of the Geology of Switzerland, 1st edition, Wepf, Basel, Switzerland, (1980), 102p.

Verma, S.P., and Santoyo, E.: New improved equations for Na/K, Na/Li and SiO_2 geothermometers by outlier detection and rejection, J*ournal of Volcanology and Geothermal Research*, **79(1-2)**, (1997), 9-23.

Site name	X-Coord	Y-Coord	Elevation (a.m.s.l.)	Sampling elevation (a.m.s.l.)	Borehole depth (m)	Formation	Formation age	Meas. Temp. (°C)	TDS (mg/l)	pH	Li	Na	K	Mg	Ca	Sr	F	Cl	Br	SO_4	HCO_3	SiO_2	Ionic balance (%)	^{18}O H_2O (‰)	^{18}O SO_4 (‰)	Ref.
Berlingen	720142	281378	406.9	-9	416	Molasse	Tertiary	29		8.5	0.05	298	1.80	1.20	2.6	0.37	3.6	48.0		161		13.1		-13.10		1
Birmenstorf	660049	257455	343.7	103	241	Limestone	Triassic	25		6.9		1446	50	258	990	8.3		4433		1900		43.2		-9.88		2
Boettstein	659340	268556	347.5	185	1326	Limestone	Muschelkalk	21	6345	6.9	2.9	1100	83	199	612	11.0	2.6	1302	0.92	2624	388	20.3	-0.2	-11.16	13.70	3
				36		Limestone	Buntsandstein	27	1977	8.6	1.60	662	16.9	2.3	20.1	0.97	12.1	638	0.78	287	319	18.4	1.4	-10.08	3.83	3
				32		Limestone	Buntsandstein	27	2095	8.3	1.50	746	9.6	4.1	38.0	0.90	12.4	693	0.69	359	343	18.7	3.5	-10.15	6.92	3
				-51		Granite	Hercynian	29.5	1028	8.1	2.02	356	8.5	0.30	9.6	0.40	12.4	121	0.83	308	342	19.0	0.0	-10.05	1.16	3
				-270		Granite	Hercynian	38	1098	7.9	1.45	378	9.8	0.20	11.8	0.34	12.0	124	1.00	340	372	28.3	1.3	-10.04	-0.15	3
				-273		Granite	Hercynian	38	1095	8.0	2.5	364	10.8	0.30	11.8	0.57	12.4	131	0.88	333	387	29.6	-2.8	-10.01	-1.32	3
				-444		Granite	Hercynian	43	1302	8.3	1.35	395	8.3	0.20	8.5	0.09	12.9	142	1.20	339	372	22.5	0.6	-9.96	-0.58	2
				-978		Granite	Hercynian	60	13210	7.0		4037	45.0	2.6	870	21.0	3.6	6621		1560	93		0.0	-7.90	8.44	2
Eglisau	680800	270000	380	140	240	Molasse	Tertiary	16	2467	7.8	0.25	843	4.2	10.6	19.8	1.00	1.40	952	0.06	320	296	8.9	0.3	-9.89		4
	680820	269865	381.8	122	260	Molasse	Tertiary	16	2643	8.4	0.35	925	4.5	12.0	23.6	0.90	1.50	1260	0.59	144	250	8.8	-0.1	-9.41	14.74	4
Kaisten	644641	265624	320.4	206	1306	Limestone	Buntsandstein	17	6821	7.0	6.8	1780	37.6	56	443	12.6	2.4	2025	4.8	2083	366	8.9	-0.1	-9.03		3
				36		Conglomerate	Perm./Carbon.	24	1628	8.0	1.95	451	12.6	2.5	32.4	1.02	7.3	104	0.55	589	403	22.8	-0.3	-10.36	3.83	3
				10		Granite	Hercynian	25	1373	7.7	1.76	431	12.2	1.60	29.8	1.00	7.9	79	0.46	572	421	20.6	-2.2	-10.29	4.47	3
				-162		Granite	Hercynian	30	1350	7.6	1.98	424	11.2	1.60	31.2	0.99	8.4	61	0.35	598	380	16.9	-0.4	-10.34	2.55	3
				-499		Granite	Hercynian	42	1245	7.1	1.86	361	19.0	1.25	48.0	1.40	7.2	67	0.47	511	372	34.8	0.0	-10.32	0.68	3
				-711		Granite	Hercynian	50	1263	7.3	2.05	361	14.5	1.20	48.6	1.42	6.9	63	0.38	508	383	53	0.7	-10.61	0.54	3
				-833		Granite	Hercynian	54	1327	8.2	1.67	410	12.8	2.1	36.9	1.24	7.4	135	0.47	491	366	37.9	0.3	-10.40	0.91	3
				-952		Granite	Hercynian	58	1428	7.9	1.85	364	24.2	3.0	34.1	1.12	7.5	73	0.47	532	366	20.5	-2.3	-10.46	0.97	3
Leuggern	657634	271208	358.8	284	1689	Limestone	Muschelkalk	13.3	1146	7.5	0.14	31.6	7.5	71	180	3.1	2.2	34.3	0.08	537	263	15.7	-0.3	-9.96	13.43	3
				141		Limestone	Buntsandstein	19.4	1858	8.8	0.83	608	9.1	3.7	17.7	0.71	10.0	486	0.85	445	268	7.8	0.2	-10.39	8.68	3
				108		Granite	Hercynian	19.5	1099	8.4	0.54	385	4.7	1.90	9.6	0.53	12.9	178		338	284	16.4	0.2	-10.49	6.41	3
				-85		Granite	Hercynian	25	988	8.8	0.60	338	4.2	1.40	9.5	0.40	12.6	130	0.70	356	220	8.5	-1.8	-10.35	4.93	3
				-179		Granite	Hercynian	28	951	8.5	0.62	324	4.1	0.60	9.8	0.52	12.4	119	0.76	360	186	15.5	0.6	-10.37	3.59	3
				-346		Granite	Hercynian	34	1037	8.6	0.84	348	4.2	0.70	14.3	0.49	12.3	109	0.79	415	214	16.7	1.0	-10.52	5.10	3
				-488		Granite	Hercynian	40	1001	8.6	0.96	332	8.0	0.30	15.0	0.52	13.4	123	0.72	362	217	23.4	0.0	-10.48	4.04	3
				-564		Granite	Hercynian	42	4871	7.8	3.1	1108	13.3	2.2	424	7.4	2.9	203		3057	73	5.7	-0.2	-10.45	10.91	3
				-844		Granite	Hercynian	51	889	8.8	0.78	311	6.0	0.20	6.1	0.24	15.4	132	0.76	270	220	20.4	-0.1	-10.42	4.72	3
				-1074		Granite	Hercynian	59	1421	8.5	1.97	468	9.9	0.50	12.8	0.67	12.2	422	4.0	278	195	20.0	0.1	-10.02	3.51	3
				-1284		Granite	Hercynian	66	899	8.2	1.08	295	8.8	0.10	9.4	0.47	14.3	125	0.72	263	273	40.0	-3.9	-10.25	-0.19	3
				-1305		Granite	Hercynian	66	888	8.3	1.00	295	16.3	0.10	10.2	0.43	14.5	124	0.79	252	256	36.3	0.2			3
Lottstetten	686170	273670	405	-138	543	Limestone	Jurassic	20.4	939	8.0		240	8.5	12.5	20.0	0.75		53	0.50	70	523	10.9	4.8	-10.32	15.06	5
Reinach	612525	262126	305	-1488	1793	Limestone	Triassic	77.6	44001	5.6	6.7	14200	270	580	1400	12.1	11.0	23650	19.0	3100	696	75	0.0	-8.70		6
Rheinfelden	627650	266680	300	-300	600	Granite	Hercynian	26.9	4180	6.5		856	35.0	45.6	260	4.5		556		950	1423	49.7	3.4	-9.24		4

Site name	X-Coord	Y-Coord	Elevation (a.m.s.l.)	Sampling elevation (a.m.s.l.)	Borehole depth (m)	Formation	Formation age	Meas. Temp. (°C)	TDS (mg/l)	pH	Li	Na	K	Mg	Ca	Sr	F	Cl	Br	SO_4	HCO_3	SiO_2	Ionic balance (%)	^{18}O H_2O (‰)	^{18}O SO_4 (‰)	Ref.
Riehen	615863	270733	276.2	-1271	1547	Limestone	Triassic	71.6	17099	6.4	4.8	4850	151	192	786	11.5	3.2	7150	8.0	2810	1100	39.2	-1.4	-9.60		6
	616437	271468	285.3	-962	1247	Limestone	Triassic	64.5	14180	6.3	4.0	3900	166	168	762	9.2	2.9	5620		2340	1180	28.5	-0.1	-9.50		6
Riniken	656604	261780	385.1	-130	1800	Limestone	Keuper	38	15409	8.4	1.75	4263	54	203	585	10.9	1.00	2775	6.6	7314	204	9.9	0.1	-6.43	11.40	3
				-272		Limestone	Muschelkalk	45	14470	6.8	0.81	3998	45.5	210	874	13.5	3.1	6008	0.70	3011	283	22.8	-0.1	-10.14	14.70	3
				-422		Sandstone	Buntsandstein	50	10310	6.6	11.3	2949	102	61	496	15.8	1.20	4030	10.2	1850	765	27.5	-0.6	-6.92	13.28	3
				-580		Limestone	Perm./Carbon.	56	15584	6.9	19.2	5191	140	81	406	32.2	1.23	7888	29.2	1477	442	29.2	-0.2	-6.73	10.13	3
				-609		Conglomerate	Perm./Carbon.	57	20124	6.6	18.0	6600	155	81	467	34.0	1.04	9900	26.4	1630	677	53	0.0	-6.65	9.27	3
				-977		Conglomerate	Perm./Carbon.	70	44243	11.1	54.5	15210	1347	0.03	902	59	0.34	23452	89	1814		14.6				3
Schafisheim	653632	246757	421	-137	1892	Molasse	Tertiary	30	8705	7.8	1.90	3032	19.1	68	209	20.4	1.46	5208	20.3	5	132	7.6	0.0	-6.41		3
				-810		Limestone	Muschelkalk	57.5	15696	6.6	6.5	4700	115	184	784	18.0	4.2	6700	5.6	2850	477	35.6	2.8	-11.02	11.04	3
				-839		Limestone	Muschelkalk	57.5	15216	6.5	6.2	4490	113	174	743	16.9	3.9	6400	6.6	2805	429	34.5	0.9	-10.81	11.60	3
				-1067		Limestone	Buntsandstein	68	15843	6.6	14.4	4955	132	67	532	17.8	2.2	6405	11.6	3083	610	25.1	-0.3	-5.42	14.71	3
				-1150		Granite	Hercynian	72	7824	5.9	8.1	2360	90	29.2	293	11.4	2.1	2420	5.7	2022	876	35.5	0.6	-6.66	12.08	3
				-1467		Granite	Hercynian	85	8319	6.8	14.5	2712	168	21.0	88	15.7	7.7	3555	9.9	793	891	53	-0.4	-5.55	9.56	3
Siblingen	680090	286693	574	234	1498.6	Sandstone	Triassic	22	599	8.2	0.64	181	4.6	0.55	6.5	0.11	7.6	26.0		77.5	273	21.2	-0.2	-12.05		3
				-586		Granite	Hercynian	47	578	8.8	0.61	172	3.8	0.70	6.0	0.18	9.3	25.0		71	267	11.8	-1.3	-12.03		3
				-921		Granite	Hercynian	57	595	8.2	0.66	172	4.6	0.40	5.5		11.0	27.0		64	281	28.3	-3.3	-11.78		3
Weiach	676750	268620	369	114	2273.5	Limestone	Malm	19	6769	7.2	0.98	2275	29.2	91	148	6.9	2.7	3795	11.5	33	466	10.8	-0.3	-5.76	12.00	3
				-490		Limestone	Muschelkalk	50	3276	6.8	0.19	139	25.1	149	579	7.9	2.8	53		1990	284	45.3	0.3	-11.76	12.70	3
				-616		Limestone	Buntsandstein	53	14621	7.3	5.4	4318	81	65	457	11.1	0.87	2921	6.9	6198	544	19.2	-0.3	-8.12	15.29	3
				-747		Sandstone	Perm./Carbon.	59	36432	7.2	10.6	12165	193	189	1046	32.6	71.0	18088	71.0	4165	609	13.2	0.1	-5.32	14.34	3
				-1039		Sandstone	Perm./Carbon.	70	97336	7.2	13.1	26112	762	1006	8890	390	0.68	59750	630	264	147	2.6	0.0	-4.61	14.17	3
				-1849		Gneiss	Hercynian	112	6432	7.7	6.3	2205	70	0.10	152	4.7	5.8	3382	32.7	431	76	44.7	0.5	-8.17	0.37	3
				-1898		Gneiss	Hercynian	112	7959	8.2	8.5	2725	93	0.40	221	6.9	8.5	4312	44.0	468	73	42.8	0.1	-7.65	2.26	3
Zurich	682150	246375	420	-80	500	Molasse	Tertiary	29	1027	8.9	0.08	318	1.8	0.84	2.5	1.80	3.2	144	1.00	129	395	8.5	2.7	-11.89	12.60	4
Zurzach-Bad	663972	271224	340	-90	430	Gneiss	Hercynian	40.4	950	8.0	1.20	282	7.4	0.71	13.7	0.59	10.3	135	0.62	220	254	25.3	1.1	-10.18		4
	664020	271325	340	-129	469	Gneiss	Hercynian	41.9	892	8.0	1.14	226	6.0	0.15	21.0	1.00	9.7	123		210	265	27.6	-6.1	-10.12	1.02	4

Reference: 1. Unpublished report, 2. Gorhan and Griesser (1998), 3. Pearson et al. (1989), 4. Högl (1980), 5. Carlé (1975), 6. Hauber (1993).

Table 1: Location, geology, chemistry and oxygen isotopic data of geothermal fluids from deep boreholes in northern Switzerland. TDS means Total Dissolved Solids. Measured temperature (Meas. Temp.) refers to the aquifer temperature from which the sample was taken, directly measured during the sampling or estimated from the geothermal gradient in the borehole. Chemical analyses are given in mg/L and location refers to the Swiss kilometric coordinates in projection, in standard CH1903.